This full text paper was peer reviewed at the direction of IEEE Communications Society subject matter experts for publication in the IEEE ICC 2011 proceedings

Hop-by-hop Beamforming for Dual-hop MIMO AF Relay Networks

Gayan Amarasuriya, Chintha Tellambura and Masoud Ardakani
Department of Electrical and Computer Engineering, University of Alberta, Edmonton, AB, Canada T6G 2V4
Email: {amarasur,chintha,ardakani}@ece.ualberta.ca

***Abstract*—This paper presents a comprehensive performance analysis of dual-hop multiple-input multiple-output amplify-and-forward relay networks with hop-by-hop beamforming. The impact of practical transmission impairments; (i) feedback delays, (ii) channel estimation errors and (iii) spatially-correlated fading on the system performance is studied. Specifically, the amount of performance degradation due to these impairments are quantified analytically. To this end, a general closed-form expression for the cumulative distribution function of the end-to-end signal-to-noise ratio is derived and used to obtain the outage probability, and the average symbol error rate (SER). Further, the asymptotic outage probability and average SER are derived to obtain valuable system-design insights such as the diversity order and array gain. Numerical results are presented to show the detrimental effect of imperfect channel state information on the system performance. Further, our analyses are validated through Monte-Carlo simulations.**

I. Introduction

Cooperative multiple-input multiple-output (MIMO) relay networks are currently receiving significant research interest and being investigated for emerging wireless system standards such as IEEE 802.16m WiMAX and Long Term Evolution (LTE)-Advanced [1]. Transmit beamforming can be employed to improve the performance of dual-hop MIMO relay networks, particularly because of its robustness against severe effects of fading [2]. In dual-hop MIMO relay networks, this robustness is achieved by steering the transmitted signal along the maximum eigenmodes of the source-to-relay ($S \rightarrow R$) and relay-to-destination ($R \rightarrow D$) hops. Nevertheless, a comprehensive performance analysis of hop-by-hop beamforming for dual-hop MIMO amplify-and-forward (AF) relay networks, which allows the possibility of using all MIMO-enabled terminals and considers practical transmission impairments such as spatially-correlated fading, channel estimation errors, and feedback delays, is not available in the literature.

Prior related research: Although the hop-by-hop beamforming has already been employed for dual-hop MIMO AF relay networks [3]–[6], these studies limit the relay (R) to a single-antenna terminal. In [3], the performance of beamforming for dual-hop (channel-assisted AF) CA-AF relay networks over independent Rayleigh fading channels is investigated. Reference [4] extends [3] by considering spatial correlated fading among antenna elements at the source (S) and R. Further, in [5], the performance of the system set-up in [3] is studied over Nakagami-m fading channels. Reference [6] investigates the performance of beamforming for fixed-gain AF relay networks over Nakagami-m fading channels.

In addition to the above studies, [7] analyzes the performance of dual-hop CA-AF beamforming and its equivalent systems by using several antenna configurations at S, R and destination (D). However, in all these system set-ups, at least one terminal is limited to a single antenna. Moreover, [8] studies the effect of multiple antennas at S on the outage probability by using maximal ratio transmission (MRT) for the $S \rightarrow R$ channel, and [9] extends this study to investigate the effect of feedback delays on MRT beamforming. Although the system set-ups in [8], [9] employ multiple-antennas at S, both R and D are single-antenna terminals.

Motivation and our contribution: As mentioned above, the hop-by-hop beamforming AF system models considered in [3]–[9] employ at least one single-antenna terminal. Thus, the achievable diversity and array gains in the relay channel are not optimal. Further, all the previous analyses except [9][1] make the ideal assumption of the availability of perfect CSI. In our analysis, this ideal assumption is replaced by more realistic ones, and the gaps in the performance analysis of beamforming in MIMO AF relay networks are filled by employing MIMO-enabled S, R, and D. We provide a comprehensive performance analysis, which includes exact and asymptotic end-to-end (e2e) performance metrics, and the impact of spatial correlation, outdated channel state information (CSI), and channel estimation errors on the system performance.

More specifically, in our system model, all three terminals, S, R and D, are equipped with N_s, N_r and N_d antennas, respectively. First, a closed-form expression for the cumulative distribution function (CDF) of the end-to-end SNR (e2e SNR) is derived and used to derive the outage probability and average symbol error rate (SER). In order to obtain direct insights about the valuable system-design parameters such as the diversity order and array gain, the asymptotic performance metrics, which are exact in high SNRs, are derived as well. The impact of spatially-correlated fading among antenna elements is studied. In particular, an asymptotically exact tight outage probability lower bound is derived by considering the arbitrarily correlated transmit and receive correlation matrices at each terminal. In order to quantify the amount of degradation due to antenna correlation with respect to the uncorrelated antennas, the asymptotic outage probability and average SER are also derived for correlated fading case as well. Numerical results are provided to investigate the degree of degradation of system performance due to practical transmission impairments: (i) spatially-correlated fading, (ii) feedback delays and (iii) channel estimation errors. Our results shows that the system

[1]The analysis in [9] is limited and considers the feedback delay effect on $S \rightarrow R$ for CA-AF relay networks having multiple-antenna S, and single-antenna R and D.

978-1-61284-233-2/11/$26.00 ©2011 IEEE

performance degrades significantly due to these impairments.

Notations: $\mathcal{K}_\nu(z)$ is the ν-th order Modified Bessel function of the second kind [10, Eq. (8.407.1)]. ${}_2\mathcal{F}_1(\alpha,\phi;\gamma;z)$ is the Gauss Hypergeometric function [10, Eq. (9.14.1)].

II. System Model

We consider a dual-hop AF relay network with MIMO-enabled S, R and D having N_s, N_r and N_d antennas, respectively. The channel matrices from $S \rightarrow R$ and $R \rightarrow D$ are denoted by $\mathbf{H}_l|_{l=1}^2$. The channel gain from the j-th transmit antenna to the i-th receive antenna is denoted by $h_l^{i,j}$ and is assumed to be independent and identical Rayleigh fading unless otherwise stated; $h_l^{i,j} \sim \mathcal{CN}(0,1)$. Moreover, the additive noise at the terminals is modeled as complex zero mean white Gaussian noise. All the terminals operate in the half-duplex mode, and e2e data transmission takes place in two time-slots. The direct link from $S \rightarrow D$ is assumed to be unavailable due to heavy shadowing and path-loss.

In practical MIMO beamfoming systems, the estimated channel matrices are generally perturbed by the addition of Gaussian errors due to channel estimation errors. Further, the beamforming vectors could be selected by using outdated CSI matrices due to feedback delays. The channel matrices having these two practical transmission impairments can be modeled as follows:

1) Feedback delay: In practice, the feedback channel from the receiver to transmitter experiences delays. We thus assume that the first hop beamforming vectors, $\mathbf{u}_1$ and $\mathbf{v}_1$, are selected by using the τ_1-delayed channel matrix $\mathbf{H}_1(t-\tau_1)$, and the second hop beamforming matrices, $\mathbf{u}_2$ and $\mathbf{v}_2$, by using τ_2-delayed $\mathbf{H}_2(t-\tau_2)$. By following a commonly used model, two channels can be modeled as $\mathbf{H}_l(t)|_{l=1}^2 = \rho_l \mathbf{H}_l(t-\tau_l) + \mathbf{E}_{d,l}$, where ρ_l is the normalized correlation coefficients between $h_l^{i,j}(t)$ and $h_l^{i,j}(t-\tau_l)$, and for Clarke's fading spectrum, $\rho_l = \mathcal{J}_0(2\pi f_l \tau_l)$, where f_l is the Doppler fading bandwidth [11]. Further, $\mathbf{E}_{d,l}$ is the error matrix, incurred by feedback delay, having mean zero and variance $(1-\rho_l^2)$ Gaussian entries.

2) Channel estimation errors: In general, orthogonal pilot-assisted channels estimates are perturbed by Gaussian errors and can be modeled as $\hat{\mathbf{H}}_l\Big|_{l=1}^2 = \mathbf{H}_l + \Delta\mathbf{H}_l$, where $\Delta\mathbf{H}_l$ is the error matrix having mean zero and variance $\sigma_{e,l}^2$ Gaussian entries. Thus, the estimated channel matrix $\hat{\mathbf{H}}_l$ is Gaussian distributed with mean zero and variance $1+\sigma_{e,l}^2$. Further, $\hat{h}_l^{i,j}$ and $h_l^{i,j}$ are jointly Gaussian distributed with a normalized correlation coefficient of $1/\sqrt{1+\sigma_{e,l}^2}$. The actual channel matrices can be written in terms of their estimates as $\mathbf{H}_l|_{l=1}^2 = \varepsilon_l \hat{\mathbf{H}}_l + \mathbf{E}_{e,l}$, where $\varepsilon_l = 1/(1+\sigma_{e,l}^2)$, and $\mathbf{E}_{e,l}$ is the Gaussian error matrix having mean zero and variance $\sigma_{e,l}^2/(1+\sigma_{e,l}^2)$ [12].

The above two channel models can readily be expressed in a general form as follows:

$$\mathbf{H}_l|_{l=1}^2 = \vartheta_l \hat{\mathbf{H}}_l + \xi_l \mathbf{E}_l, \tag{1}$$

where $\mathbf{H}_l$ and $\hat{\mathbf{H}}_l$ are the actual and estimated channel matrices, and $\mathbf{E}_l$ is the error matrix, and all three have zero mean and unit variance i.i.d. Gaussian entries. The parameters ϑ_l and ξ_l account for the channel estimate quality and can be explicitly given for the two cases: (i) feedback delays: $\vartheta_l = \rho_l$ and $\xi_l = \sqrt{1-\rho_l^2}$, and (ii) channel estimation errors: $\vartheta_l = 1/\sqrt{1+\sigma_{e,l}^2}$ and $\xi_l = \sqrt{\sigma_{e,l}^2/(1+\sigma_{e,l}^2)}$.

In the first time-slot, S transmits the symbol $\mathcal{X}$, having $\mathcal{E}\{|\mathcal{X}|^2\}$ =1, and R receives Y_R as

$$\begin{aligned} Y_R &= \hat{\mathbf{u}}_1^H\Big[\sqrt{\mathcal{P}_1}\mathbf{H}_1\hat{\mathbf{v}}_1\mathcal{X} + \mathbf{n}_1\Big] \\ &= \hat{\mathbf{u}}_1^H\Big[\sqrt{\mathcal{P}_1}\Big(\vartheta_1\hat{\mathbf{H}}_1 + \xi_1\mathbf{E}_1\Big)\hat{\mathbf{v}}_1\mathcal{X} + \mathbf{n}_1\Big] = \vartheta_1\sqrt{P_1\hat{\lambda}_1}\mathcal{X} + \hat{\mathbf{n}}_R, \end{aligned} \tag{2}$$

where $\hat{\mathbf{u}}_1$ and $\hat{\mathbf{v}}_1$ are the transmit precoding and receive filtering (beamforming) vectors[2] at S and R, and selected by using the imperfect channel matrix $\hat{\mathbf{H}}_1$ as the first columns of $\hat{\mathbf{U}}_1$ and $\hat{\mathbf{V}}_1$, respectively, corresponding to the largest singular value of $\hat{\mathbf{H}}_1$. Here $\mathcal{P}_1$ is the transmit power at S and $\hat{\mathbf{n}}_R$ can be considered as the effective Gaussian noise component having mean zero and variance $\sigma_{\hat{n}_R}^2 = \mathcal{P}_1\xi_1^2 + \sigma_1^2$ [12]. Further, $\hat{\lambda}_1$ is the largest eigenvalue of the Wishart matrix $\hat{\mathbf{H}}_1^H\hat{\mathbf{H}}_1$. In the second time-slot, R amplifies the received signal Y_R with a gain G and forwards to D again by using beamforming. The signal received at D, Y_D is thus given by

$$Y_D = \hat{\mathbf{u}}_2^H[G\mathbf{H}_2\hat{\mathbf{v}}_2 Y_R + \mathbf{n}_2] = G\vartheta_1\vartheta_2\sqrt{\mathcal{P}_1\hat{\lambda}_1\hat{\lambda}_2}\mathcal{X} + \hat{\mathbf{n}}_D, \tag{3}$$

where $\mathcal{P}_2$ is the transmit power at R and $\hat{\mathbf{n}}_D$ is the effective Gaussian noise component having mean zero and variance $\sigma_{\hat{n}_D}^2 = G^2\mathcal{P}_1\hat{\lambda}_1\vartheta_1^2\xi_2^2 + G^2\hat{\lambda}_2\vartheta_2^2\sigma_{\hat{n}_R}^2 + G^2\xi_2^2\sigma_{\hat{n}_R}^2 + \sigma_2^2$. Again, the beamforming vectors $\mathbf{u}_2$ and $\mathbf{v}_2$ are selected by using the imperfect channel matrix $\hat{\mathbf{H}}_2$ as the first columns of $\hat{\mathbf{U}}_2$ and $\hat{\mathbf{V}}_2$. Further, $\hat{\lambda}_2$ is the largest eigenvalues of Wishart matrix $\hat{\mathbf{H}}_2\hat{\mathbf{H}}_2^H$. After some trivial mathematical manipulations, the e2e SNR γ_{eq} can be derived as

$$\gamma_{eq} = \frac{\vartheta_1^2\mathcal{P}_1\hat{\lambda}_1\vartheta_2^2\hat{\lambda}_2}{\mathcal{P}_1\hat{\lambda}_1\vartheta_1^2\xi_2^2 + \hat{\lambda}_2\vartheta_2^2\sigma_{\hat{n}_R}^2 + \xi_2^2\sigma_{\hat{n}_R}^2 + \frac{\sigma_2^2}{G^2}}. \tag{4}$$

Now, the relay gain in (4) is set to $G_1 = \sqrt{\mathcal{P}_2/(\mathcal{P}_1\hat{\lambda}_1 + \sigma_1^2)}$, and the e2e SNR can be derived as

$$\gamma_{eq} = \frac{\gamma_1\gamma_2}{\alpha\gamma_1 + \gamma_2 + \beta}, \tag{5}$$

where $\alpha = \frac{\mathcal{P}_2\xi_2^2\vartheta_1^2 + \sigma_2^2}{\vartheta_1^2(\mathcal{P}_2\xi_2^2+\sigma_2^2)}$, and $\beta = \frac{\mathcal{P}_2\xi_2^2(\mathcal{P}_1\xi_1^2+\sigma_1^2)+\sigma_1^2\sigma_2^2}{(\mathcal{P}_1\xi_1^2+\sigma_1^2)(\mathcal{P}_2\xi_2^2+\sigma_2^2)}$. Further, $\gamma_1 = \frac{\mathcal{P}_1\vartheta_1^2\hat{\lambda}_1}{\mathcal{P}_1\xi_1^2+\sigma_1^2}$ and $\gamma_2 = \frac{\mathcal{P}_2\vartheta_2^2\hat{\lambda}_2}{\mathcal{P}_2\xi_2^2+\sigma_2^2}$ are the instantaneous SNRs of $S \rightarrow R$ and $R \rightarrow D$ hops having average SNRs $\bar{\gamma}_1 = \frac{\mathcal{P}_1\vartheta_1^2}{\mathcal{P}_1\xi_1^2+\sigma_1^2}$ and $\bar{\gamma}_2 = \frac{\mathcal{P}_2\vartheta_2^2}{\mathcal{P}_2\xi_2^2+\sigma_2^2}$.

Alternatively, if the relay has the knowledge of the channel estimation error variance and long-term feedback channel statistics (i.e., ϑ_1 and ξ_1), then the relay gain can be set to $G_2 = \sqrt{\mathcal{P}_2/(\mathcal{P}_1\vartheta_1^2\hat{\lambda}_1 + \mathcal{P}_1\xi_1^2 + \sigma_1^2)}$. Now, (4) can further be simplified to obtain the e2e SNR as $\gamma_{eq} = \frac{\gamma_1\gamma_2}{\gamma_1+\gamma_2+1}$, where γ_1 and γ_2 are defined as in (5). Further, (5) can handle the perfect CSI cases when $\rho_l|_{l=1}^2 = 1$ and $\sigma_{e,l}^2\Big|_{l=1}^2 = 0$.

[2]The singular value decompositions of $\hat{\mathbf{H}}_1$ and $\hat{\mathbf{H}}_2$ are given by $\hat{\mathbf{H}}_1 = \hat{\mathbf{U}}_1\hat{\mathbf{\Sigma}}_1\hat{\mathbf{V}}_1^H$ and $\hat{\mathbf{H}}_2 = \hat{\mathbf{U}}_2\hat{\mathbf{\Sigma}}_2\hat{\mathbf{V}}_2^H$. Here $\hat{\mathbf{\Sigma}}_1$ and $\hat{\mathbf{\Sigma}}_2$ are $N_r \times N_s$ and $N_d \times N_r$ diagonal matrices having the largest singular values $\sqrt{\lambda_1}$ and $\sqrt{\lambda_2}$, as the first elements on the main diagonals, respectively. Further, $\hat{\mathbf{U}}_1$, $\hat{\mathbf{V}}_1$, $\hat{\mathbf{U}}_2$ and $\hat{\mathbf{V}}_2$ are unitary square matrices of sizes $N_r \times N_r$, $N_s \times N_s$, $N_d \times N_d$, and $N_r \times N_r$.

III. Performance Analysis

In this section, the performance analysis is presented. First, the statistics of the e2e SNR are derived and used to derive the performance metrics.

A. Statistical characterization of the end-to-end SNR

The exact CDF of the e2e SNR (5) is given by (see Appendix for the proof)

$$F_{\gamma_{eq}}(x) = 1 - \sum_{a,b,k,l,m} \sum_{u=0}^{m} \sum_{v=0}^{b} \frac{2\alpha^u \binom{m}{u}\binom{b}{v} d_1(a,b) d_2(k,l)}{b!\; m! (a)^{\frac{u+v-m-2b-1}{2}}} \times \frac{(k)^{\frac{u+v+m+1}{2}} x^{\frac{m+2b+u-v+1}{2}} (\alpha x+\beta)^{\frac{m-u+v+1}{2}}}{(\bar{\gamma}_1)^{\frac{2b-u-v+m+1}{2}} (\bar{\gamma}_2)^{\frac{u+v+m+1}{2}}} \times \mathrm{e}^{-x\left(\frac{a}{\bar{\gamma}_1}+\frac{\alpha k}{\bar{\gamma}_2}\right)} \mathcal{K}_{u+v-m+1}\left(2\sqrt{\frac{akx(\alpha x+\beta)}{\bar{\gamma}_1\bar{\gamma}_2}}\right), \quad (6)$$

where $\sum_{a,b,k,l.m} = \sum_{a=1}^{\min(N_s,N_r)} \sum_{b=|N_s-N_r|}^{(N_s+N_r)a-2a^2} \sum_{k=1}^{\min(N_r,N_d)} \sum_{l=|N_r-N_d|}^{(N_r+N_d)k-2k^2} \sum_{m=0}^{l}$ and the coefficients $d_l(i,j)|_{l=1}^{2}$ satisfy $d_l(i,j) = \sum_{i=1}^{\min(N,M)} \sum_{j=|N-M|}^{(N+M)i-2i^2} d_l(i,j) = 1$ and can readily be computed by using the efficient algorithm in [13].

B. Outage probability

The outage probability P_{out} is the probability that the instantaneous e2e SNR γ_{eq} falls below a threshold γ_{th}. Thus, P_{out} can be obtained as $P_{out} = \Pr(\gamma_{eq} \le \gamma_{th}) = F_{\gamma_{eq}}(\gamma_{th})$, where $F_{\gamma_{eq}}(\gamma_{th})$ denotes the CDF of γ_{eq} (6) evaluated at γ_{th}.

C. Average symbol error rate

The average SER $\bar{P}_e$ can be derived by averaging the conditional error probability (CEP) $P_{e|\gamma}(\gamma)$ over the PDF of the e2e SNR; $\bar{P}_e = \mathcal{E}_{\gamma_{eq}}\left[P_{e|\gamma}(\gamma)\right]$. The CEP for a wide range of modulation schemes is given by $P_{e|x}(x) = \eta \mathcal{Q}(\sqrt{\zeta\gamma})$, where η and ζ are modulation-dependent constants. By using integration by parts, $\bar{P}_e$ can be simplified as $\bar{P}_e = \frac{\eta}{2}\sqrt{\frac{\zeta}{2\pi}} \int_0^\infty x^{-\frac{1}{2}} \mathrm{e}^{-\frac{\zeta x}{2}} F_{\gamma_{eq}}(x)\,\mathrm{d}x$. An asymptotically exact lower bound for the average SER is derived by substituting (6) with $\beta = 0$ into the integral representation of $\bar{P}_e$ and evaluating the integral by using [10, Eq. (6.621.3)] as

$$\bar{P}_e^{lb} = \frac{\eta}{2} - \frac{\eta}{2}\sqrt{\frac{\zeta}{2}} \sum_{a,b,k,l,m} \sum_{u=0}^{m+b} \frac{2\binom{m+b}{u} d_1(a,b) d_2(k,l)}{b!\; m! (a)^{\frac{u-m-2b-1}{2}}} \times \frac{(\alpha k)^{\frac{u+m+1}{2}}}{(\bar{\gamma}_1)^{\frac{2b-u+m+1}{2}} (\bar{\gamma}_2)^{\frac{u+m+1}{2}}} \mathbb{I}(\mu,\nu,\psi,\omega), \quad \text{where} \quad (7)$$

$\mu = m+b+\frac{3}{2}$, $\nu = u-m+1$, $\psi = \frac{\zeta}{2} + \frac{a}{\bar{\gamma}_1} + \frac{\alpha k}{\bar{\gamma}_2}$, $\omega = 2\sqrt{\frac{a\alpha k}{\bar{\gamma}_1\bar{\gamma}_2}}$.

1) Asymptotic outage probability: To obtain direct insights, the asymptotic outage probability can be derived as

$$P_{out}^{\infty} = \begin{cases} \Omega_1 \left(\frac{x}{\bar{\gamma}}\right)^{N_s N_r} + o\left(\bar{\gamma}^{-(N_s N_r+1)}\right), & N_s < N_d \\ \Omega_2 \left(\frac{x}{\bar{\gamma}}\right)^{N N_r} + o\left(\bar{\gamma}^{-(N N_r+1)}\right), & N_s = N_d = N \\ \Omega_3 \left(\frac{x}{\bar{\gamma}}\right)^{N_d N_r} + o\left(\bar{\gamma}^{-(N_d N_r+1)}\right), & N_s > N_d, \end{cases} \quad (8)$$

where $\Omega_1 = \frac{\Gamma_{n_1}(n_1)}{\Gamma_{n_1}(m_1+n_1)(k_1)^{N_s N_r}}$, $\Omega_2 = \frac{\Gamma_{n_1}(n_1)}{\Gamma_{n_1}(m_1+n_1)(k_1)^{N N_r}} + \frac{\Gamma_{n_2}(n_2)}{\Gamma_{n_2}(m_2+n_2)(k_2)^{N N_r}}$, and $\Omega_3 = \frac{\Gamma_{n_2}(n_2)}{\Gamma_{n_2}(m_2+n_2)(k_2)^{N_d N_r}}$. Here $\Gamma_a(b) = \prod_{i=1}^{a} \Gamma(b-i+1)$ is the normalized complex multivariate gamma function. Further, $m_1 = \max(N_s, N_r)$, $m_2 = \max(N_r, N_d)$, $n_1 = \min(N_s, N_r)$, and $n_2 = \min(N_r, N_d)$.

2) Asymptotic average SER: In the high SNR regime, the average SER can be approximated as $\bar{P}_e^{\infty} = (\bar{\gamma} G_a)^{-G_d}$, where G_d is the diversity order, and G_a is the array gain. By using (8) and the integral expression of $\bar{P}_e$ in Section III-C, the asymptotic average BER is derived as

$$\bar{P}_e^{\infty} = \begin{cases} \frac{\Omega_1 \eta 2^{N_s N_r - 1}\Gamma(N_s N_r + \frac{1}{2})}{\sqrt{\pi}(\zeta\bar{\gamma})^{N_s N_r}} + o\left(\bar{\gamma}^{-(N_s N_r+1)}\right), & N_s < N_d \\ \frac{\Omega_2 \eta 2^{N N_r - 1}\Gamma(N N_r + \frac{1}{2})}{\sqrt{\pi}(\zeta\bar{\gamma})^{N N_r}} + o\left(\bar{\gamma}^{-(N N_r+1)}\right), & N_s = N_d = N \\ \frac{\Omega_3 \eta 2^{N_r N_d - 1}\Gamma(N_r N_d + \frac{1}{2})}{\sqrt{\pi}(\zeta\bar{\gamma})^{N_r N_d}} + o\left(\bar{\gamma}^{-(N_r N_d+1)}\right), & N_s > N_d. \end{cases} \quad (9)$$

Now, by using (8) and (9), the diversity order and array gain are obtained as $G_d = N_r \min(N_s, N_d)$ and $G_a = \left(\frac{\Omega_l \eta 2^{G_d-1}\Gamma(G_d+\frac{1}{2})}{\sqrt{\pi}(\zeta)^{G_d}}\right)^{-\frac{1}{G_d}}$, where $\Omega_l|_{l=1}^{3}$ stands for the three cases defined in (8).

D. Impact of correlated fading among antenna elements

In this section, the impact of correlated fading among the antenna elements of S, R and D on the system performance is investigated. Assume that $\mathbf{H}_1$ and $\mathbf{H}_2$ undergo flat spatially arbitrary-correlated Rayleigh fading. Then $\mathbf{H}_1$ and $\mathbf{H}_2$ can be decomposed according to the Kronecker correlation structure as follows: $\mathbf{H}_1 = \Upsilon_1^{\frac{1}{2}} \tilde{\mathbf{H}}_1 \Phi_1^{\frac{1}{2}}$ and $\mathbf{H}_2 = \Upsilon_2^{\frac{1}{2}} \tilde{\mathbf{H}}_2 \Phi_2^{\frac{1}{2}}$, where Υ_1 and Υ_2 are the transmit correlation matrices at S and R, and Φ_1 and Φ_2 are the receive correlation matrices at R and D, respectively. Further, $\tilde{\mathbf{H}}_1 \sim \mathcal{CN}(0_{N_r \times N_r}, \mathbf{I}_{N_r} \otimes \mathbf{I}_{N_s})$ and $\tilde{\mathbf{H}}_2 \sim \mathcal{CN}(0_{N_d \times N_r} \mathbf{I}_{N_d} \otimes \mathbf{I}_{N_r})$.

1) CDF of the e2e SNR: The exact CDF of the e2e SNR is mathematically intractable. However, the CDF of an asymptotically exact upper bound of the e2e SNR can be derived. By using the SNR upper bound, $\gamma_{eq} \le \gamma_{eq}^{\text{ub}} = \min(\gamma_1, \gamma_2)$, the CDF of γ_{eq}^{ub} can be derived as $F_{\gamma_{eq}^{\text{ub}}}(x) = 1 - (1 - F_{\gamma_1}(x))(1 - F_{\gamma_2}(x))$, where $F_{\gamma_1}(x)$ and $F_{\gamma_2}(x)$ are the CDFs of the first and second hop SNRs and given by [14]

$$F_{\gamma_l}(x)|_{l=1}^{2} = \left.\frac{(-1)^{n_l}\Gamma_{n_l}(n_l)\det(\Upsilon_l)^{n_1-1}\det(\Phi_l)^{m_1-1}\det\left(\Psi_l\left(\frac{x}{\gamma_l}\right)\right)}{\Delta_{n_l}(\Upsilon_l)\Delta_{m_l}(\Phi_l)\,(x/\gamma_l)^{n_l(n_l-1)/2}}\right|_{l=1}^{2} \quad (10)$$

where $\Delta_k(\cdot)$ is a Vandermonde determinant in the eigenvalues of the k-dimensional matrix argument, and the (i,j)-th element of $\Psi_l(x)$ is given by [14, Eq. (1)]. By evaluating $F_{\gamma_{eq}^{\text{ub}}}(x)$ at γ_{th}, a tight outage probability lower bound can readily be derived.

2) High SNR analysis: In order to quantify the amount of performance degradation due to spatial correlated fading, the asymptotic outage probability and average SER are derived. The asymptotic outage probability, when each channel undergoes correlated fading, can be derived by replacing $\Omega_l|_{l=1}^{3}$ in (8) with

$$\Omega' = \begin{cases} \Omega_1' = \frac{\Gamma_{n_1}(n_1)}{\det(\Upsilon_1)^{m_1}\det(\Psi_1)^{n_1}\Gamma_{n_1}(m_1+n_1)(k_1)^{N_s N_r}}, & N_s < N_d \\ \Omega_2' = \frac{\Gamma_{n_1}(n_1)}{\det(\Upsilon_1)^{m_1}\det(\Psi_1)^{n_1}\Gamma_{n_1}(m_1+n_1)(k_1)^{N N_r}} & \\ \quad + \frac{\Gamma_{n_2}(n_2)}{\det(\Upsilon_2)^{m_2}\det(\Psi_2)^{n_2}\Gamma_{n_2}(m_2+n_2)(k_2)^{N N_r}}, & N_s = N_d = N \\ \Omega_3' = \frac{\Gamma_{n_2}(n_2)}{\det(\Upsilon_2)^{m_2 v}\det(\Psi_2)^{n_2}\Gamma_{n_2}(m_2+n_2)(k_2)^{N_d N_r}}, & N_s > N_d. \end{cases} \quad (11)$$

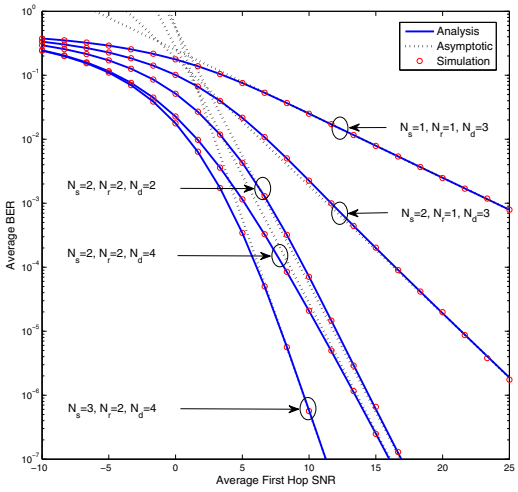

Fig. 1. The average BER of BPSK of MIMO beamforming AF relay networks. The hop distances are $L_1 = 2L_2$ and the path-loss exponent is $\varpi = 2.5$.

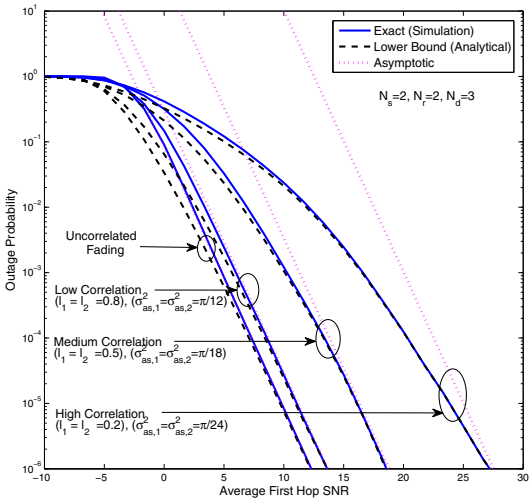

Fig. 2. The impact of spatial correlation on the outage probability. The hop distances are $L_1 = L_2$, and the path-loss exponent is $\varpi = 2.5$.

The asymptotic average SER can readily be derived again by substituting the above $\Omega_l'|_{l=1}^{3}$ into (9). Although the diversity order of the system remains the same regardless of the amount of correlation, the array gain significantly reduces with respect to the uncorrelated fading by factors of Ω_1/Ω_1', Ω_2/Ω_2', and Ω_3/Ω_3' for the cases $N_s \leq N_d$, $N_s = N_d$, and $N_s \geq N_d$, respectively (see Section IV).

IV. Numerical Results

This section presents the numerical results and verifies our analysis through Monte-Carlo simulations. To capture the effect of the network geometry, the average SNR of the i-th hop is modeled as $\bar{\gamma}_i|_{i=1}^{2} = \bar{\gamma}\left(\frac{L_0}{L_i}\right)^{\varpi}$, where $\bar{\gamma}$ is the average transmit SNR, L_0 is the reference distance, and ϖ is the path-loss exponent. The distances between the terminals $S \rightarrow R$, and $R \rightarrow D$ are denoted by L_1 and L_2, respectively.

1) Diversity order and array gain: In Fig. 1, the average bit error rate (BER) of binary phase shift keying (BPSK) is plotted for the perfect CSI case ($\rho_l = 1$ and $\sigma_{e,l}^2 = 0$). An ideal CA-AF relay ($\alpha = 1, \beta = 0$ in (5)) is treated and the BER curves are plotted by using (7). The asymptotic average BER curves are also plotted to depict the valuable system-design parameters such as the diversity order and array gain. The asymptotic BER curves clearly show the diversity gains obtained by different antenna set-ups at each terminal. Specifically, the asymptotic BER curves corresponding to $N_s = 2, N_r = 2, N_d = 2$, and $N_s = 2, N_r = 2, N_d = 4$ reveal that the diversity order of both set-ups is the same ($G_d = 4$), and thus verify our diversity analysis $G_d = N_r \min(N_s, N_d)$. However, the latter network set-up experiences a higher array gain than that of the former because of the two additional antennas at D.

2) Impact of correlated fading on the outage probability: Fig. 2 shows the effect of correlated fading among the antennas at S, R and D on the outage probability. The transmit and receive arbitrary correlation matrices Υ_1, Υ_2, Ψ_1 and Ψ_2 for uniform linear antenna arrays at S, R and D are constructed by using [15, Eq. (4)]. The amount of spatial correlation between

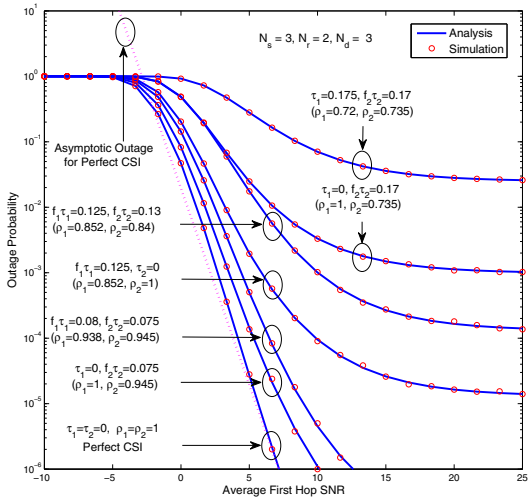

Fig. 3. The impact of outdated CSI on the outage probability. The hop distances are $L_1 = 2L_2$ and the path-loss exponent is $\varpi = 2.5$.

adjacent antenna elements then can be quantified by using their relative antenna spacing (l_1, l_2), angular spreads $(\sigma_{as,1}^2, \sigma_{as,2}^2)$, and the angle of arrival or departure (θ_1, θ_2). Three different correlation scenarios are obtained as (a) high correlation, (b) medium correlation, and (c) low correlation. Since l_1 and l_2 are the relative antenna spacing, and $\sigma_{as,1}^2$ and $\sigma_{as,2}^2$ are the angular spreads, smaller values of l_1, l_2, $\sigma_{as,1}^2$ and $\sigma_{as,2}^2$ result in higher spatial correlation [15]. The asymptotic outage curves reveal that the amount of correlation does not affect the attainable diversity order, but the array gain is severely affected by higher correlation. Our outage lower bounds are tighter in moderate-to-high SNR regimes, asymptotically exact at high SNRs, and provide valuable system-design insights.

3) Impact of outdated CSI on the outage probability: In Fig. 3, the impact of outdated CSI due to feedback delay on the outage probability is shown. The relay does not have the knowledge of feedback channel statistics ρ_l. The beamforming vectors at S, R and D are selected based on the outdated CSI received via the local feedback channels $R \rightarrow S$ and $D \rightarrow R$ with time delays τ_1 and τ_2. Several outage curves

are obtained by changing ρ_1 and ρ_2, where they are related to the time delays by following Clarke's fading model. Thus, $\rho_1 = \mathcal{J}_0(2\pi f_1 \tau_1)$ and $\rho_2 = \mathcal{J}_0(2\pi f_2 \tau_2)$, where f_1 and f_2 are the Doppler fading frequencies. The outage performance degrades significantly even when the feedback channels experience slight time delays. In fact, the achievable diversity gain diminishes completely whenever there exists even a slight time delay in either the $R \to S$ or $D \to R$ feedback channel.

4) Impact of channel estimation errors on the average BER: Fig. 4 depicts the effect of channel estimation errors on the average BER of BPSK. The channels $S \to R$ and $R \to D$ are modeled by using (1). Even a slight estimation error in either channel degrades the BER performance significantly. When the estimation error is assumed to be fixed, the BER curves exhibit error floors as the average first hop SNR increases. However, in practice, the estimation errors are inversely propositional to the pilot symbol SNR, $\sigma_{e,l}^2 \propto \left(\frac{E_p}{\sigma_l^2}\right)\Big|_{l=1}^{2}$, where E_p is the pilot symbol power and σ_l^2 is the noise variance. Specifically, when the variance of the Gaussian estimation errors decreases as the SNR of the data symbols increases (the pilot symbols have the same energy as the data symbols), the error floors do not occur and the achievable diversity order is persevered; however, the array gain is severely degraded. Two types of relay gains, G_1 and G_2, are treated. Specifically, G_1 does not have the knowledge of channel estimation error variance $\sigma_{e,l}^2$, whereas G_2 does. Fig. 4 shows that the relays having the knowledge of $\sigma_{e,l}^2$ always perform the best.

V. Conclusion

The performance of hop-by-hop beamforming for dual-hop MIMO AF relay networks was studied. The effect of spatially-correlated fading, feedback delays and channel estimation errors on the system performance was derived, thereby quantifying the amount of performance degradation. Our results show that these practical transmission impairments result in significant performance degradations. Valuable system-design parameters such as the diversity order and array gains were derived by using our asymptotic analysis of performance metrics. Our analytical and simulation results provide valuable insights for designing practical dual-hop MIMO relay networks with beamforming.

VI. Appendix

The CDF of γ_{eq} in (5) can be derived by using $F_{\gamma_{eq}}(x) = 1 - \int_0^\infty \bar{F}_{\gamma_2}\left(\frac{(\alpha(x+z)+\beta)x}{z}\right) f_{\gamma_1}(z+x)\mathrm{d}z$, where $f_{\gamma_1}(x)$ is the PDF of γ_1 and $\bar{F}_{\gamma_2}(x)$ is the complementary CDF of γ_2. In order to derive $F_{\gamma_{eq}}(x)$, one needs the closed-form statistics of $\hat{\lambda}_1$ and $\hat{\lambda}_2$, the largest eigenvalues of the central Wishart matrices. By using [2], $f_{\gamma_1}(x)$ can be obtained as

$$f_{\gamma_2}(x) = \sum_{a=1}^{\min(N_s,N_r)} \sum_{b=|N_s-N_r|}^{(N_s+N_r)a-2a^2} \frac{a^{b+1} d_1(a,b)}{(\bar{\gamma}_1)^{b+1}\,(b)!} x^b \mathrm{e}^{-\frac{ax}{\bar{\gamma}_1}}. \quad (12)$$

Similarly, $\bar{F}_{\gamma_2}(x)$ can readily be derived as

$$\bar{F}_{\gamma_1}(x) = \sum_{k=1}^{\min(N_r,N_d)} \sum_{l=|N_r-N_d|}^{(N_r+N_d)k-2k^2} \sum_{m=0}^{l} \frac{k^m d_2(k,l)}{(\bar{\gamma}_2)^m\,(m)!} x^m \mathrm{e}^{-\frac{kx}{\bar{\gamma}_2}}, \quad (13)$$

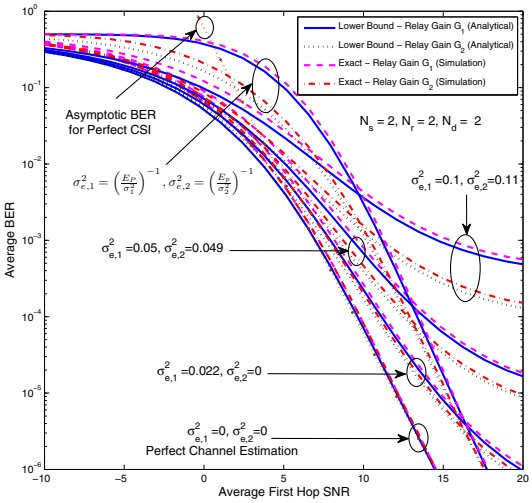

Fig. 4. The impact of channel estimation errors on the average BER of BPSK. The hop distances are $L_1 = 0.75L_2$ and the path-loss exponent is $\varpi = 2.5$.

where $d_1(a,b)$ and $d_2(k,l)$ are defined in (6). Now, by substituting (12) and (13) into the integral representation of $F_{\gamma_{eq}}(x)$ and evaluating the integral by using [10, Eq. (3.471.9)], the desired result in (6) can be derived.

References

[1] Y. Yang *et al.*, "Relay technologies for WiMAX and LTE-Advanced mobile systems," *IEEE Commun. Mag.*, vol. 47, pp. 100–105, Oct. 2009.

[2] P. Dighe *et al.*, "Analysis of transmit-receive diversity in Rayleigh fading," *IEEE Trans. Commun.*, vol. 51, no. 4, pp. 694–703, Apr. 2003.

[3] R. H. Y. Louie *et al.*, "Performance analysis of beamforming in two hop amplify and forward relay networks," in *Proc. IEEE Int. Conf. on Commun.*, May 19–23, 2008, pp. 4311–4315.

[4] ——, "Performance analysis of beamforming in two hop amplify and forward relay networks with antenna correlation," *IEEE Trans. Wireless Commun.*, vol. 8, no. 6, pp. 3132–3141, Jun. 2009.

[5] T. Duong *et al.*, "Symbol error probability of hop-by-hop beamforming in Nakagami-m fading," *Electronics Letters*, vol. 45, no. 20, pp. 1042–1044, Sep. 2009.

[6] D. da Costa and S. Aissa, "Cooperative dual-hop relaying systems with beamforming over Nakagami-m fading channels," *IEEE Trans. Wireless Commun.*, vol. 8, no. 8, pp. 3950–3954, Aug. 2009.

[7] J.-B. Kim and D. Kim, "Performance of dual-hop amplify-and-forward beamforming and its equivalent systems in Rayleigh fading channels," *IEEE Trans. Commun.*, vol. 58, no. 3, pp. 729–732, Mar. 2010.

[8] H. Min *et al.*, "Effect of multiple antennas at the source on outage probability for amplify-and-forward relaying systems," *IEEE Trans. Wireless Commun.*, vol. 8, no. 2, pp. 633–637, Feb. 2009.

[9] H. Suraweera *et al.*, "Effect of feedback delay on downlink amplify-and-forward relaying with beamforming," in *IEEE GLOBECOM 2009.*, Nov. 2009.

[10] I. Gradshteyn and I. Ryzhik, *Table of integrals, Series, and Products*, 7th ed. Academic Press, 2007.

[11] S. Zhou and G. Giannakis, "Adaptive modulation for multi-antenna transmissions with channel mean feedback," *IEEE Trans. Wireless Commun.*, vol. 3, no. 5, pp. 1626–1636, Sep. 2004.

[12] Y. Chen and C. Tellambura, "Performance analysis of maximum ratio transmission with imperfect channel estimation," *IEEE Commun. Lett.*, vol. 9, no. 4, pp. 322 – 324, Apr. 2005.

[13] A. Maaref and S. Aissa, "Closed-form expressions for the outage and ergodic Shannon capacity of MIMO MRC systems," *IEEE Trans. Commun.*, vol. 53, no. 7, pp. 1092–1095, Jul. 2005.

[14] M. McKay *et al.*, "Performance analysis of MIMO-MRC in double-correlated Rayleigh environments," *IEEE Trans. Commun.*, vol. 55, no. 3, pp. 497–507, Mar. 2007.

[15] H. Bolcskei *et al.*, "Impact of the propagation environment on the performance of space-frequency coded MIMO-OFDM," *IEEE J. Sel. Areas Commun.*, vol. 21, pp. 427–439, Apr. 2003.